Available online at www.sciencedirect.com
ScienceDirect
Journal of Solid State Chemistry 180 (2007) 1519–1525
JOURNAL OF SOLID STATE CHEMISTRY
www.elsevier.com/locate/jssc

Anisotropic thermal expansion and hydrogen bonding behavior of portlandite: A high-temperature neutron diffraction study

H. Xu[a,b,*], Y. Zhao[b], S.C. Vogel[b], L.L. Daemen[b], D.D. Hickmott[a]

[a]*Earth and Environmental Sciences Division, Los Alamos National Laboratory, Los Alamos, NM 87545, USA*
[b]*Los Alamos Neutron Science Center, Los Alamos National Laboratory, Los Alamos, NM 87545, USA*

Received 11 January 2007; received in revised form 26 February 2007; accepted 2 March 2007
Available online 12 March 2007

Abstract

The structure of deuterated portlandite, $Ca(OD)_2$, was investigated using time-of-flight neutron diffraction in the temperature range 308–643 K. Rietveld analysis reveals that with increasing temperature, the *c* dimension expands at a rate ~4.5 times larger than that for *a*. This anisotropy of thermal expansion is due to rapid increase in the interlayer thickness along *c* with increasing temperature. Fitting of the measured cell volumes yields a coefficient of thermal expansion, $\alpha = \alpha_0 + \alpha_1 T$, where $\alpha_0 = 5.966 \times 10^{-5}\,K^{-1}$ and $\alpha_1 = 3.333 \times 10^{-8}\,K^{-2}$. On heating, hydrogen-mediated interatomic interactions within the interlayer become weakened, as reflected by increases in the interlayer D⋯O and D⋯D distances with increasing temperature. Correspondingly, the three equivalent sites over which D is disordered become further apart, suggesting a more delocalized configuration of D at high temperatures.

Keywords: Portlandite; Neutron diffraction; Thermal expansion; Hydrogen bonding; Crystal chemistry

1. Introduction

Portlandite [$Ca(OH)_2$], a member of the layered hydroxide family (space group $P\bar{3}m1$), is composed of edge-sharing [CaO_6] octahedral layers parallel to (001) with hydrogen bonding between the layers (Fig. 1) [1]. Within the interlayer, each H interacts with three O–H bonds from the neighboring [CaO_6] layer through H⋯O attraction and H⋯H repulsion. These unique structural features make $Ca(OH)_2$, together with other $M(OH)_2$ layered hydroxides, a model system for studying hydrogen-mediated interactions, which are among the most common interatomic interactions in physical and biological systems. $M(OH)_2$ compounds are also interesting from a geological viewpoint, since they are present as component units in the structures of complex hydrous minerals, which are potential hosts for water in the Earth's mantle [2–4]. Thus studying their structures and stability will provide insights into the mechanisms of water storage in the deep Earth. Moreover, portlandite is of importance in the cement industry because it is one of the major phases in cement paste, a hydration product of Portland cement. Thus the proportion of portlandite in cement paste and its response to changing temperature and/or other conditions during the curing process will ultimately affect the strength and durability of concrete. To better utilize cement/concrete for various applications, an accurate determination of the stability and properties of portlandite such as its thermal expansion coefficients is necessary.

Most structural studies of portlandite have treated hydrogen as occupying a single site, $\left(\frac{1}{3}, \frac{2}{3}, z\right)$, similar to oxygen, thereby forming O–H bonds along the *c*-axis. In this model, H exhibits very large anisotropic displacement parameters in the (001) plane, which Busing and Levy [1] described as a "riding" motion of H relative to O. Desgranges et al. [5] proposed an alternative, three-site split-atom model to describe the hydrogen positions based on their results from single-crystal neutron diffraction. Specifically, H is displaced from the 3-fold symmetry axis and disorders over three positions with occupancy of $\frac{1}{3}$ about the 3-fold rotation (Fig. 1). More recently, using *ab initio* molecular simulation, Raugei et al. [6] demonstrated that portlandite adopts the three-site split-hydrogen model

*Corresponding author. Fax: +1 505 665 2676.
E-mail address: hxu@lanl.gov (H. Xu).

0022-4596/$ - see front matter © 2007 Elsevier Inc. All rights reserved.
doi:10.1016/j.jssc.2007.03.004

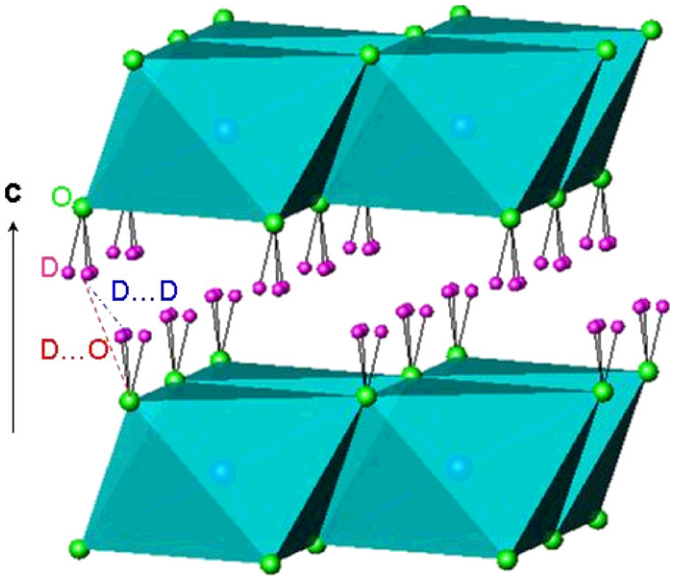

Fig. 1. Crystal structure of portlandite. Octahedra represent [CaO_6] units, green balls represent O atoms, and pink balls represent $H(D)$ atoms. Note that each $H(D)$ atom is disordered over three positions about the 3-fold rotation with occupancy of $\frac{1}{3}$. Red and blue dash lines indicate the interlayer D···O and D···D distances, respectively.

at high pressure and, further, the distance between the three sites increases with increasing pressure. This model has also been used to interpret neutron diffraction results for other hydroxides such as brucite, $Mg(OH)_2$ [7–9], β-$Co(OH)_2$ [10] and β-$Ni(OD)_2$ [11]. However, as most of the structural studies on portlandite used X-ray diffraction, where H is a weak scatterer, they simply treated hydrogen as occupying the single $\left(\frac{1}{3}, \frac{2}{3}, z\right)$ site. Furthermore, despite a number of diffraction studies of portlandite at high temperature and pressure, measurements of its coefficients of thermal expansion (CTEs) are surprisingly scarce [12–15], and the detailed mechanisms of thermal expansion remain largely unclear. Since changes in cell dimensions with temperature are likely to be coupled with changes in the hydrogen bonding behavior and since neutron scattering is sensitive to the position of hydrogen (and its isotopes), high-temperature neutron diffraction studies of portlandite are particularly useful to unravel its thermal expansion mechanisms.

In this study, we carried out *in situ* neutron diffraction of portlandite using a pulsed neutron source at temperatures up to 643 K (the sample started to decompose into CaO plus water vapor at 613 K). To avoid the large incoherent scattering of neutrons by hydrogen, we synthesized deuterated portlandite, $Ca(OD)_2$, via hydration of CaO with D_2O. Rietveld analysis of the time-of-flight neutron data allowed determination of structural parameters as a function of temperature. In particular, the atomic positions and displacement parameters of D at high temperatures have been obtained, and implications for D motion and D-mediated interactions as well as their effects on thermal expansion are discussed.

2. Experimental methods

2.1. Sample synthesis

The portlandite sample used in this study was prepared via hydration of CaO powders with D_2O. First, CaO powders were obtained by heat-treating $CaCO_3$ powders (Alfa Aesar, 99.95%) at 1233 K for ~5 h with the emitted CO_2 gas constantly pumped out. Second, the CaO powders were slowly added to boiling D_2O in a custom-built, sealed reaction line to minimize possible reaction of CaO with CO_2 from air. Third, the resulted sample was dried at ~373 K under vacuum and stored in a desiccator. The product, a white, well-crystallized powder, was confirmed to be portlandite by powder X-ray diffraction (Rigaku Ultima III, 40 keV, 50 mA, Cu$K\alpha$ radiation).

2.2. Neutron diffraction

Time-of-flight neutron diffraction experiments were performed at the High-Pressure Preferred Orientation (HiPPO) beamline of the Manuel Lujan Jr. Neutron Scattering Center, Los Alamos National Laboratory [16,17]. Sample powders were placed in a vanadium can 0.95 cm in diameter, and the can was mounted in an ILL-type high-temperature furnace with vanadium heating elements and heatshields for contamination-free diffraction data collection [17]. Data were collected under vacuum at 308 K and then at temperatures from 343 to 643 K with an interval of 30 K. For each temperature point, three detector banks with nominal diffraction angles of 40°, 90° and 140° were simultaneously used. The heating rate was 5 K/min, and the dwell time at each targeted temperature (including an equilibration time of 5 min) was ~3 h.

2.3. Structure refinement

The neutron data were analyzed using the Rietveld method with the General Structure Analysis System (GSAS) program of Larson and Von Dreele [18]. The starting structural parameters for $Ca(OD)_2$ at 308 K were taken from the single-crystal neutron diffraction study of Desgranges et al. [5]. We then used the refined structural parameters at 308 K as the starting parameters for the next highest temperature and continued this procedure systematically with increasing temperature. For the two highest temperature runs (613 and 643 K), since a small portion of the sample decomposed into CaO and water vapor, we included CaO as a secondary phase in our Rietveld analysis. For each temperature point, two data sets from the detectors at $2\theta = 90°$ and 140° were simultaneously analyzed (the 40° data set was not used because of its relatively low resolution). The refinements proceeded as follows: after the scale factor and four background terms (Shifted Chebyshev function) for each histogram had converged, lattice parameters, zero points and phase fractions (for the runs at 613 and 643 K) were added and

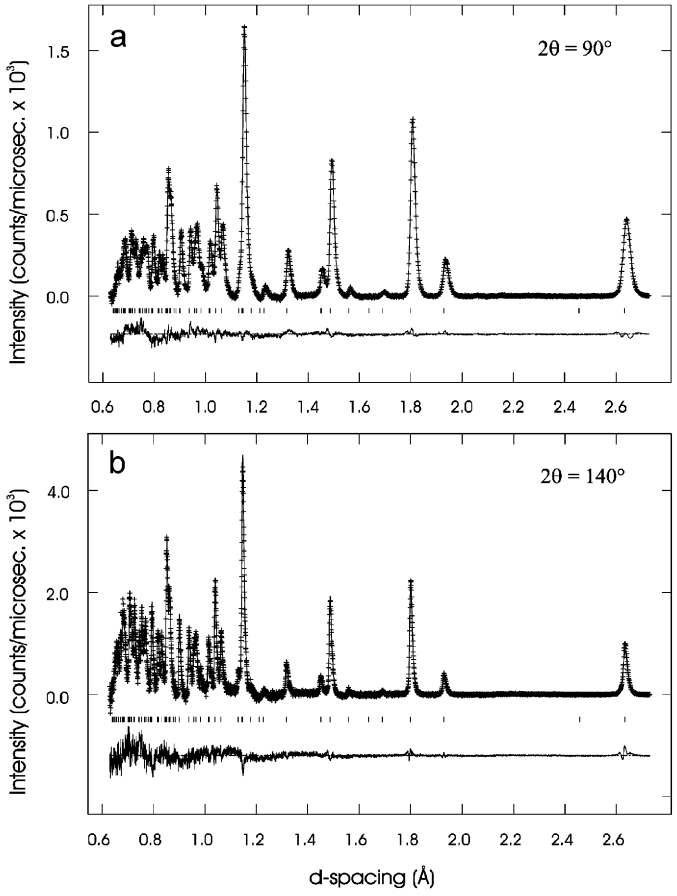

Fig. 2. A pair of fitted neutron diffraction patterns of $Ca(OD)_2$ collected at (a) $2\theta = 90^\circ$ and (b) $2\theta = 140^\circ$ at 308 K. Data are shown as plus signs, and the solid curve is the best fit to the data. Tick marks below the pattern show the positions of allowed reflections, and the lower curve represents the difference between the observed and calculated profiles.

optimized. Fourteen or 18 additional background terms were then added for each histogram, and the peak profiles were fitted to a TOF profile function [19]. On convergence of the preceding parameters, atomic coordinates and isotropic atomic displacement parameters for Ca, O and D were refined. A representative pair of fitted patterns is plotted in Fig. 2.

3. Results and discussion

Our high-temperature neutron diffraction patterns indicate that the $Ca(OD)_2$ sample was stable from 308 to 583 K. However, it started to decompose into CaO and D_2O(g) when the temperature reached 613 K (the molar ratio CaO:$Ca(OD)_2$ obtained from the Rietveld analysis is 1.2:98.8). Thus the onset temperature of the dehydroxylation (T_d) lies between 583 and 613 K. As demonstrated in previous studies, the dehydroxylation temperature of portlandite increases with increasing water vapor pressure (P_{water}). For example, T_d changes from 488 K under vacuum to 580 K at $P_{water} = 1.8$ Torr and to 783 K at $P_{water} = 1$ atm [20,21]. The T_d of our sample is within the above range, consistent with the relatively low vapor pressure within the sample can (the sample can was not well sealed).

Table 1
Agreement indices of the refinements using different $Ca(OD)_2$ models

	Single-site D model		Three-site D model	
	U_{iso}	U_{aniso}	U_{iso}	U_{aniso}
R_{wp}(%)	1.21	1.12	1.13	1.11
R_p (%)	0.97	0.91	0.91	0.89
χ^2	3.67	3.15	3.18	3.06

As stated earlier, two structure models have been used to describe the position of H (D) in portlandite: the single-site $\left(\frac{1}{3}, \frac{2}{3}, z_D\right)$ model with D located on the 3-fold rotation axis and the three-site (x_D, $2x_D$, z_D) model with D disordered over three equivalent positions about the 3-fold symmetry axis. We used both models to analyze the data collected at 308 K, with isotropic (U_{iso}) or anisotropic (U_{aniso}) displacement parameters refined (Table 1). For the single-site model, using U_{aniso} gave a significantly better fit to the observed pattern than using U_{iso} ($\chi^2 = 3.15$ for using U_{aniso} compared with $\chi^2 = 3.67$ for using U_{iso}). For the three-site model, using U_{iso} and U_{aniso} gave similar values of refinement agreement indices, but the latter yielded unreasonable U values, presumably because the resolution of the data is not high enough to refine more parameters. The closeness of the agreement indices based on the single-site, U_{aniso} model and the three-site, U_{iso} model (Table 1) suggests a correlation between the coordinate (x, y, z) of D and its displacement parameters U. However, it is beyond the scope of this study to determine which model is more appropriate to describe the hydrogen positions, due to the limited resolution of the data. Nevertheless, using high-resolution single-crystal neutron diffraction, Desgranges et al. [5] demonstrated the validity of the three-site split-atom model. Thus for the subsequent analyses of the high-temperature data, only the three-site, U_{iso} model was employed. The obtained unit-cell parameters, atomic coordinates and atomic displacement parameters, and selected interatomic distances are listed in Tables 2–4, respectively.

3.1. Thermal expansion

On heating, both unit-cell parameters a and c increase, and thus cell volume V also increases (Fig. 3). However, as shown in Figs. 3a and b, the structural expansion occurs at a much higher rate along the c-axis than along the a-axis and is thus highly anisotropic, which is consistent with the layered nature of its structure [10,12]. To obtain the mean CTEs, we fitted the cell-parameter data to linear relations:

$$a = 3.5876 + 4.2339 \times 10^{-5} T \quad (R^2 = 0.999), \tag{1}$$

$$c = 4.8303 + 2.5800 \times 10^{-4} T \quad (R^2 = 0.999), \tag{2}$$

Table 2
Unit-cell parameters of $Ca(OD)_2$ and agreement indices of the refinements

T (K)	a (Å)	c (Å)	V (Å^3)	R_{wp} (%)	χ^2
308	3.60045(9)	4.9113(2)	55.136(4)	1.13	3.18
343	3.60214(7)	4.9189(2)	55.274(3)	0.84	4.68
373	3.60352(7)	4.9269(2)	55.406(3)	0.83	4.54
403	3.60483(8)	4.9345(2)	55.532(3)	0.82	4.45
433	3.60600(8)	4.9415(2)	55.647(3)	0.80	4.23
463	3.60725(8)	4.9491(2)	55.771(3)	0.79	4.05
493	3.60822(8)	4.9560(2)	55.878(3)	0.79	3.99
523	3.60966(8)	4.9642(2)	56.016(3)	0.76	4.27
553	3.61096(9)	4.9723(2)	56.148(3)	0.77	3.86
583	3.6122(1)	4.9809(2)	56.282(3)	0.77	3.75
613	3.6136(1)	4.9894(2)	56.423(3)	0.73	3.38
643	3.6150(1)	4.9978(2)	56.560(4)	0.74	3.40

Table 3
Atomic coordinates[a] and isotropic atomic displacement parameters[b] of $Ca(OD)_2$ (space group $P\bar{3}m1$)

T (K)	z(O)	x(D)	z(D)	U_{iso}(Ca)	U_{iso}(O)	U_{iso}(D)
308	0.2339(2)	0.3665(4)	0.4252(2)	0.55(4)	1.16(3)	2.40(5)
343	0.2334(1)	0.3677(3)	0.4232(2)	0.87(4)	1.33(3)	2.60(4)
373	0.2330(2)	0.3688(3)	0.4221(2)	1.03(4)	1.46(3)	2.91(5)
403	0.2327(2)	0.3694(4)	0.4208(2)	1.11(4)	1.65(3)	3.21(5)
433	0.2326(2)	0.3700(4)	0.4200(2)	1.22(4)	1.80(3)	3.43(6)
463	0.2322(2)	0.3703(4)	0.4192(3)	1.32(4)	1.94(3)	3.74(6)
493	0.2318(2)	0.3709(4)	0.4080(3)	1.44(5)	2.06(3)	3.96(6)
523	0.2314(2)	0.3715(4)	0.4169(3)	1.57(5)	2.23(3)	4.19(7)
553	0.2311(2)	0.3717(5)	0.4163(3)	1.59(5)	2.43(4)	4.42(7)
583	0.2305(3)	0.3729(5)	0.4148(3)	1.79(5)	2.51(4)	4.59(8)
613	0.2301(3)	0.3728(5)	0.4140(4)	1.84(5)	2.71(4)	4.91(8)
643	0.2298(3)	0.3736(6)	0.4131(4)	2.10(6)	2.86(4)	5.1(1)

[a] $x(Ca) = y(Ca) = z(Ca) = 0$; $x(O) = \frac{1}{3}$; $y(O) = \frac{2}{3}$; $y(D) = 2x(D)$.
[b] The unit of U_{iso}: Å^2/100.

Table 4
Selected interatomic distances of $Ca(OD)_2$

T (K)	Ca–O (Å)	O–O (Å)[a]	D–D (Å)	O–D (Å)	D···D (Å)	D···O (Å)
308	2.3751(4)	3.099(1)	0.358(4)	0.962(1)	2.115(1)	2.511(2)
343	2.3755(4)	3.098(1)	0.371(3)	0.958(1)	2.120(1)	2.517(2)
373	2.3762(4)	3.098(1)	0.383(4)	0.957(1)	2.123(1)	2.519(2)
403	2.3770(4)	3.099(1)	0.390(4)	0.955(1)	2.127(1)	2.523(2)
433	2.3781(4)	3.101(1)	0.397(4)	0.954(1)	2.130(1)	2.526(2)
463	2.3787(5)	3.102(1)	0.400(4)	0.954(1)	2.133(1)	2.531(2)
493	2.3789(5)	3.101(2)	0.406(4)	0.953(1)	2.137(2)	2.536(3)
523	2.3797(5)	3.102(2)	0.413(5)	0.951(1)	2.141(2)	2.541(3)
553	2.3804(6)	3.103(2)	0.415(5)	0.952(2)	2.144(2)	2.545(3)
583	2.3807(6)	3.102(2)	0.429(5)	0.951(2)	2.148(2)	2.549(3)
613	2.3813(6)	3.102(2)	0.428(5)	0.950(2)	2.153(2)	2.557(3)
643	2.3821(8)	3.103(2)	0.437(6)	0.951(2)	2.156(2)	2.560(4)

[a] The length of the O–O edge shared by two $[CaO_6]$ octahedra.

$$V = 53.825 + 4.2185 \times 10^{-3} T \quad (R^2 = 0.999). \tag{3}$$

The derived mean CTEs of $Ca(OD)_2$ in the temperature range 308–643 K are: $\alpha_a = 1.1759 \times 10^{-5}\,K^{-1}$; $\alpha_c = 5.2548 \times 10^{-5}\,K^{-1}$; and $\alpha_V = 7.6527 \times 10^{-5}\,K^{-1}$. Thus the

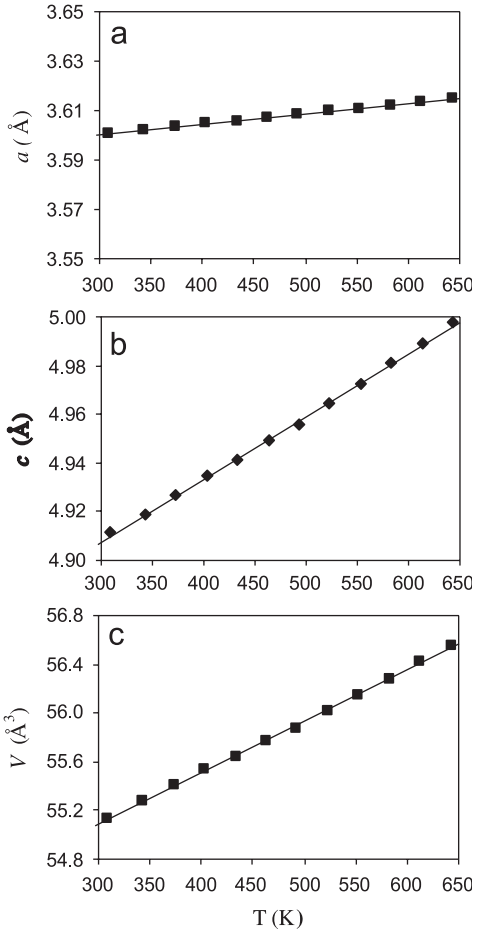

Fig. 3. Variation of unit-cell parameters (a) a, (b) c, and (c) cell volume V of $Ca(OD)_2$ with temperature. The lines are the best fits to the data.

c-axis expands ~4.5 times more rapidly than the a-axis with temperature.

The larger axial thermal expansion along c can be explained in terms of the structure. As described earlier, the portlandite structure is composed of (001) $[CaO_6]$ octahedral sheets that are held together via H-mediated dispersive forces (Fig. 1). The cell parameter c can be treated as the sum of the thickness of the $[CaO_6]$ layer and of the interlayer. With increasing temperature, the $[CaO_6]$ layer thickness only shows a slight increase, whereas the interlayer spacing increases rapidly (Fig. 4). This behavior is due apparently to the much weaker forces between neighboring $[CaO_6]$ sheets than within the sheets themselves.

The cell volume data can also be fitted to a more general equation for thermal expansion:

$$V(T) = V_0 \exp[\int \alpha(T)\,dT], \tag{4}$$

where V_0 is the volume at a chosen reference temperature, T_0, and $\alpha(T)$ is the thermal expansion coefficient, having the form:

$$\alpha(T) = \alpha_0 + \alpha_1 T. \tag{5}$$

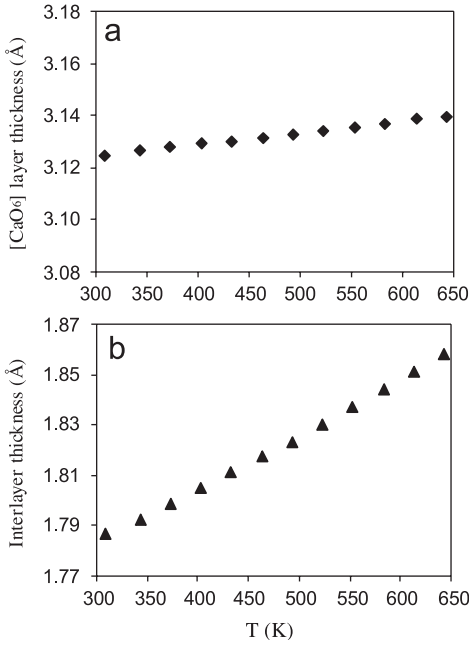

Fig. 4. Variation of (a) [CaO_6] layer thickness and (b) interlayer spacing of $Ca(OD)_2$ as a function of temperature.

Using $T_0 = 308$ K, the fit yielded the following parameters: $V_0 = 55.143(7)$ Å^3, $\alpha_0 = 5.966 \times 10^{-5}$ K^{-1}, and $\alpha_1 = 3.333 \times 10^{-8}$ K^{-2}. This fit is excellent, as indicated by an R^2 value of 0.9996 and that the refined V_0 is essentially the same as the measured V_0 [55.136(4) Å3] within the errors.

We note that our determined α_0 and α_1 values are quite different from those of Fukui et al. [15] obtained using conventional X-ray diffraction ($\alpha_0 = 3.4184 \times 10^{-7}$ K^{-1}, and $\alpha_1 = 1.2736 \times 10^{-7}$ K^{-2}). Other previous studies of portlandite used different formulae of thermal expansion and did not provide lists of cell parameters or volumes, prohibiting direct comparison of their CTEs with our α_0 and α_1 values. Nevertheless, disparities between measured CTEs may occur due to differences in sample crystallinity, in number of measurements, in the pressure of water vapor surrounding the sample (which affects the dehydroxylation temperature of portlandite and thus the temperature range in which the volumes were measured), and in systematic errors associated with diffraction techniques (laboratory X-rays vs. neutrons). Note that determination of lattice parameters (and thus cell volume) in Fukui et al. was done by conventional least-squares analysis of selected individual reflection lines, rather than the more accurate whole-pattern Rietveld method, which was used in this study.

3.2. Hydrogen behavior

Since H is the atom through which adjacent [CaO_6] layers are held together, the thickening of the interlayer with increasing temperature must be caused by corresponding changes in the H-mediated interatomic interactions. Fig. 5 shows variation of isotropic displacement factors

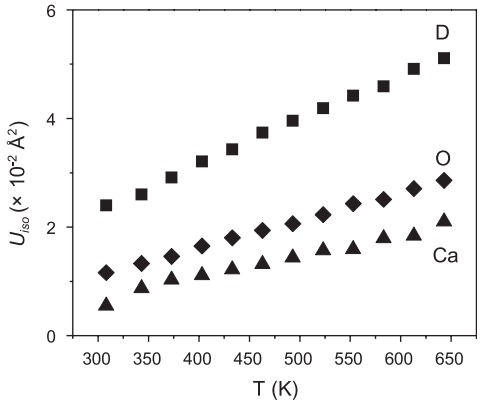

Fig. 5. Variation of isotropic atomic displacement parameters (U_{iso}) of Ca, O and D in $Ca(OD)_2$ with temperature.

(U_{iso}) of Ca, O and D with temperature. At a given temperature, $U_{iso}(Ca) < U_{iso}(O) < U_{iso}(D)$. Further, the rate of increase in U_{iso} with increasing temperature becomes larger in the sequence: $(\partial U_{iso}/\partial T)(Ca) < (\partial U_{iso}/\partial T)(O) < (\partial U_{iso}/\partial T)(D)$. These trends are consistent with the decreased bond strengths from Ca to O to D (with their neighboring atoms), as $U(= kT/f$, where k is the Boltzman constant, T absolute temperature, and f the bond force constant [22]) is inversely proportional to the bond force constant. In particular, because D only has weak electrostatic interactions with the adjacent D and O, it exhibits much larger U_{iso} and $\partial U_{iso}/\partial T$ than the more tightly bonded Ca and O.

The evolution of the thermal vibration of D on heating must be closely related to changes in its interactions with the neighboring D and O. At room temperature, D is disordered over three sites symmetrically distributed about the 3-fold rotation with occupancy of $\frac{1}{3}$, rather than being on the rotation axis itself (Fig. 1). With increasing temperature, the distance between these three equivalent sites increases (Fig. 6a), indicating a more delocalized configuration of D with respect to the single $(\frac{1}{3}, \frac{2}{3}, z)$ site. Correspondingly, the D⋯O attraction (Fig. 1), which operates between a given D and its closest O from the neighboring [CaO_6] layer, becomes weakened, as manifested by the increase in D⋯O distance (Fig. 6b). A similar trend is seen in the variation of D⋯D (Fig. 6c), the distance between two nearest non-bonded D atoms associated with adjacent [CaO_6] layers (Fig. 1). Hence, both the attractive D⋯O and the repulsive D⋯D interactions become weakened with increasing temperature, a direct consequence of the increased interlayer spacing (Fig. 4b). In contrast, the O–D bond length shows small decreases on heating (Fig. 6d), suggesting that the O–D bond may become somewhat stronger (though the shorter O–D distances might also be a result of not taking into account the possibly larger anisotropic displacement parameters of D in the (001) plane at higher temperatures). Because the interlayer D⋯O distance increases with increasing temperature, the bonding contribution of

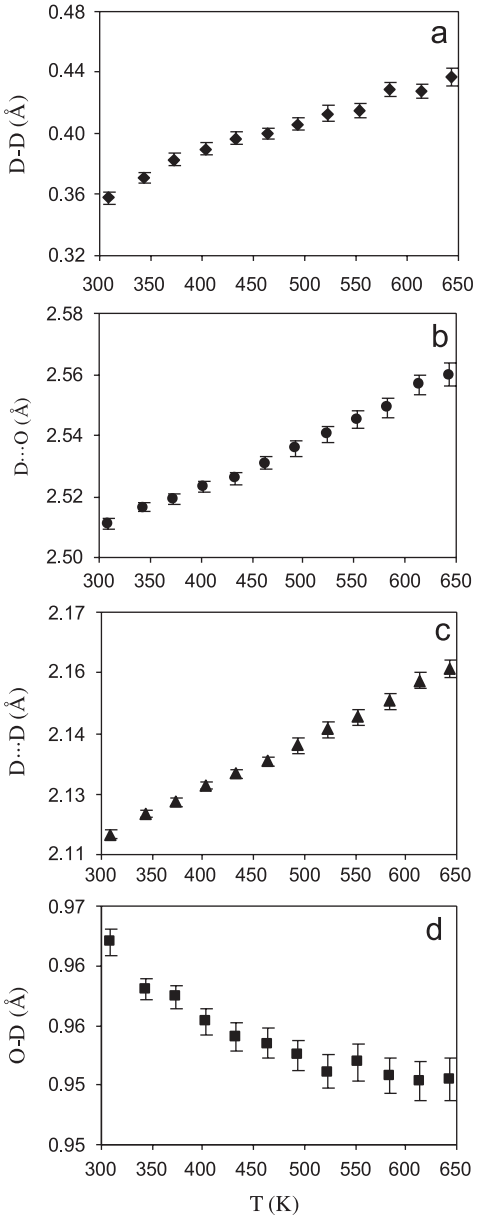

Fig. 6. Variation of interatomic distances (a) D–D, (b) D···O, (c) D···D and (d) O–D in $Ca(OD)_2$ as a function of temperature.

D···O in the D···O–D configuration becomes weakened. To compensate the D···O weakening, the O–D bond may become shortened and thus strengthened, in accordance with the bond valence arguments [23]. Hence, the interatomic interactions of D with its neighboring D and O (which are associated with the same or different $[CaO_6]$ layers) are interdependent and are driven by the thermal motion of D at elevated temperatures.

Chaix-Pluchery and Niepce [24] reported the so-called "prereactional transformations" in portlandite, which can occur more than a hundred degrees before its dehydroxylation. These transformations are characterized by slope changes in the temperature dependences of lattice parameter c, O–H bond length, and/or interlayer H–H distance. The authors attributed these variations in structural parameters to lattice disorder/distortion in the stacking of (001) $[CaO_6]$ layers, which interacts strongly with point defects possibly formed due to proton jumping on heating. However, the trends in our measured lattice parameters, U_{iso} values and interatomic distances (Figs. 3, 5 and 6) are continuous throughout the temperature range 308–643 K, even as the $Ca(OD)_2$ sample starts to decompose at 613 K. This behavior suggests that the effect of dehydroxylation on the portlandite structure is minimal. The occurrence/lack of the "prereactional transformations" may largely depend on the water vapor pressure used in the experiments. As described earlier, the vacuum or very low vapor pressure conditions used in Chaix-Pluchery et al.'s study led to the dehydroxylation occurring at much lower temperatures (e.g., 488 K under vacuum compared with 783 K at 1 atm) [20]. Because of the same energetic favorability, these conditions may cause non-uniform motion of H and formation of H_2O or O^{2-} on the OH^- sites, thereby creating point defects (including vacancies due to the escape of H_2O from the OH^- sites [24]) and triggering corresponding structural changes. To reveal the detailed mechanisms of the "prereactional transformations", however, more structural analyses (such as by high-temperature inelastic neutron scattering) at various water vapor pressures are needed.

4. Conclusions

We have studied the high-temperature structural behavior of $Ca(OD)_2$ using neutron diffraction in conjunction with Rietveld analysis up to its dehydroxylation point. With increasing temperature, both the a and c dimensions expand, but the latter at a rate ~4.5 times larger. The larger expansion along c is due to the weak D-mediated interatomic interactions within the interlayer and thus the ease of changing its thickness. At a given temperature, the amplitude of thermal vibration of D is much larger than those for Ca and O, and, further, it increases more rapidly with increasing temperature. On heating, the interlayer D···O and D···D distances increase, implying weakened D-mediated interactions between the $[CaO_6]$ layers. Moreover, the distance between the three partially occupied D sites also increases, and thus D becomes more delocalized relative to the single $\left(\frac{1}{3}, \frac{2}{3}, z\right)$ site at elevated temperatures.

Acknowledgments

We are grateful to J. William Carey and the anonymous reviewers for helpful comments and Patrick Woodward for handling this paper. This work has benefited from the use of the Lujan Neutron Scattering Center at LANSCE, which is funded by the Department of Energy's Office of Basic Energy Sciences. Los Alamos National Laboratory is operated by Los Alamos National Security, LLC, under DOE Contract DE-AC52-06NA25396.

References

[1] W.R. Bushing, H.A. Levy, J. Chem. Phys. 26 (1957) 563.
[2] C.T. Prewitt, J.B. Parise, In: R.M. Hazen, R.T. Downs (Eds.), High-Temperature and High-Pressure Crystal Chemistry, Reviews in Mineralogy and Geochemistry, Vol. 41, 2000, p. 307.
[3] M.B. Kruger, Q. Williams, R. Jeanloz, J. Chem. Phys. 91 (1989) 5910.
[4] Y. Fei, H.-K. Mao, J. Geophys. Res. 98 (1993) 11875.
[5] L. Desgranges, D. Grebille, G. Calvarin, Acta Crystallogr. B 49 (1993) 812.
[6] S. Raugei, P.L. Silvestrelli, M. Parrinello, Phys. Rev. Lett. 83 (1999) 2222.
[7] J.B. Parise, K. Leinenweber, D.J. Weidner, K. Tan, Am. Min. 79 (1994) 193.
[8] L. Desgranges, G. Calvarin, G. Chevrier, Acta Crystallogr. B 52 (1996) 82.
[9] B.C. Chakoumakos, C.K. Loong, A.J. Schultz, J. Phys. Chem. B 101 (1997) 9458.
[10] J.B. Parise, J.S. Loveday, R.J. Nelmes, H. Kagi, Phys. Rev. Lett. 83 (1999) 328.
[11] J.B. Parise, H. Cox, H. Kagi, R. Li, W. Marshall, J.S. Loveday, S. Klotz, High Press. Sci. Technol. 7 (1998) 211.
[12] O. Chaix-Pluchery, J. Pannetier, J. Bouillot, J.C. Niepce, J. Solid State Chem. 67 (1987) 225.
[13] L. Desgranges, D. Grebille, G. Calvarin, N. Floquet, J.C. Niepce, Phase Transitions 31 (1991) 283.
[14] L. Desgranges, D. Grebille, G. Calvarin, K. Chhor, C. Pommier, N. Floquet, J.C. Niepce, J. Phys. Chem. Solids 55 (1994) 161.
[15] H. Fukui, O. Ohtaka, T. Fujisawa, T. Kunisada, T. Suzuki, T. Kikegawa, High Press. Res. 23 (2003) 55.
[16] H.R. Wenk, L. Lutterotti, S.C. Vogel, Nucl. Instrum. Methods Phys. Res. A 515 (2003) 575.
[17] S.C. Vogel, C. Hartig, L. Lutterotti, R.B. Von Dreele, H.R. Wenk, D.J. Williams, Powder Diffract. 19 (2004) 65.
[18] A.C. Larson, R.B. Von Dreele, GSAS—General Structure Analysis System, Los Alamos National Laboratory Report No. LAUR 86-748, 2000.
[19] R.B. Von Dreele, J.D. Jorgensen, C.G. Windsor, J. Appl. Cryst. 15 (1982) 581.
[20] O. Chaix-Pluchery, J. Bouillot, D. Closmak, J.C. Niepce, F. Freund, J. Solid Sate Chem. 50 (1983) 247.
[21] T.B. Bai, A.F. Koster van Groos, S. Guggenheim, Am. Min. 79 (1994) 1223.
[22] R.M. Hazen, L.W. Finger, Comparative Crystal Chemistry, Wiley, New York, 1982.
[23] I.D. Brown, Acta Crystallogr. B 48 (1992) 553.
[24] O. Chaix-Pluchery, J.C. Niepce, Reactivity Solids 5 (1988) 69.